ORIGINAL ARTICLE

Myocardial ultrastructure can augment genetic testing for sporadic dilated cardiomyopathy with initial heart failure

Tsunenori Saito[1,2]* (ID), Naoko Saito Sato[3], Kosuke Mozawa[2], Akiko Adachi[4], Yoshihiro Sasaki[4], Kotoka Nakamura[1], Eiichiro Oka[2], Toshiaki Otsuka[5], Eitaro Kodani[6], Kuniya Asai[7], Kyoichi Mizuno[2], Wataru Shimizu[2] and Roberta A. Gottlieb[1]

[1]*Smidt Heart Institute, Cedars-Sinai Medical Center, 8700 Beverly Blvd, Los Angeles, CA 90048, USA;* [2]*Department of Cardiovascular Medicine, Nippon Medical School Graduate School, Tokyo, Japan;* [3]*Department of Neurology, Japanese Red Cross Medical Center, Tokyo, Japan;* [4]*Division of Morphological and Biomolecular Research, Graduate School of Medicine, Nippon Medical School, Tokyo, Japan;* [5]*Department of Hygiene and Public Health, Nippon Medical School Graduate School, Tokyo, Japan;* [6]*Department of Internal Medicine and Cardiology, Nippon Medical School Tama Nagayama Hospital, Tokyo, Japan; and* [7]*Intensive Care Unit, Nippon Medical School Chiba Hokusoh Hospital, Chiba, Japan*

Abstract

Aims   The aim of the present study was to consider whether the ultrastructural features of cardiomyocytes in dilated cardiomyopathy can be used to guide genetic testing.
Methods and results   Endomyocardial biopsy and whole-exome sequencing were performed in 32 consecutive sporadic dilated cardiomyopathy patients [51.0 (40.0–64.0) years, 75% men] in initial phases of decompensated heart failure. The predicted pathogenicity of ultrarare (minor allele frequency ≤0.0005), non-synonymous variants was determined using the American College of Medical Genetics guidelines. Focusing on 75 cardiomyopathy-susceptibility and 41 arrhythmia-susceptibility genes, we identified 404 gene variants, of which 15 were considered pathogenic or likely pathogenic in 14 patients (44% of 32). There were five sarcomeric gene variants (29% of 17 variants) found in five patients (16% of 32), involving a variant of *MYBPC3* and four variants of *TTN*. A patient with an *MYBPC3* variant showed disorganized sarcomeres, three patients with *TTN* variants located in the region encoding the A-band domain showed sparse sarcomeres, and a patient with a *TTN* variant in encoding the I-band domain showed disrupted sarcomeres. The distribution of diffuse myofilament lysis depended on the causal genes; three patients with the same *TMEM43* variant had diffuse myofilament lysis near nuclei ($P = 0.011$), while two patients with different *DSP* variants had lysis in the peripheral areas of cardiomyocytes ($P = 0.033$).
Conclusions   Derangement patterns of myofilament and subcellular distribution of myofilament lysis might implicate causal genes. Large-scale studies are required to confirm whether these ultrastructural findings are related to the causative genes.

Introduction

Dilated cardiomyopathy (DCM) is a severe heart disease characterized by enlarged ventricles and systolic dysfunction.[1] DCM is a major cause of heart failure (HF) and heart

transplantation (HTx). In some patients with DCM, optimal treatments for HF such as renin–angiotensin system inhibitors and beta-blockers can gradually improve left ventricular (LV) function and prognosis.[2] Recently, the causative genes of several diseases have been detected by next-generation

sequencing. *TTN*[3] and *LMNA*,[4] have been reported to be involved in DCM, with associations between gene variants and clinical features such as prognosis[5] and deterioration of cardiac function,[6] have been evaluated.

Electron microscopy of endomyocardial biopsy (EMB) samples allows the detailed analysis of cardiomyocyte degeneration.[7–9] Myofilament changes in cardiomyocytes[7] and abnormal nuclei[8] could predict poor prognosis, and autophagic vacuoles[9] were associated with better prognosis in DCM patients. Ultrastructural alterations were expected to have some relationships to variants in genes encoding myocardial constitutive proteins; however, direct association between individual gene variants and ultrastructural findings in patients with DCM has not been thoroughly studied.

A period-specific observational study[10] showed that early diagnosis and intervention of DCM improved prognosis. Identification of the causative gene for DCM may lead to risk stratification of patients and enable individualized treatment; however, it is difficult to detect sporadic DCM at asymptomatic or early stages of HF. Indeed, beyond DCM, there is currently no evidence for risk reduction due to genomic medicine in routine general practice.[11] In contrast, EMB to distinguish secondary cardiomyopathy is performed relatively early as part of insured medical care in Japan. Here, we investigated whether the ultrastructural features of cardiomyocytes might augment genetic testing, such as whole-exome sequencing.

Methods

Study population

The present study enrolled 32 Japanese patients with sporadic DCM. All patients underwent DNA collection from peripheral blood and EMB from the left ventricle during the period from October 2001 to December 2011, inclusive, at the Nippon Medical School Hospital (*Figure 1*). A DCM diagnosis was made from the combined results of trans-thoracic echocardiography, coronary angiography, left ventriculography, and EMB. Patients with secondary (metabolic, drug-induced, or inflammatory) cardiomyopathies, myocarditis (according to the Dallas criteria), neuromuscular disorders, congenital, ischaemic, or severe valvular heart disease were excluded. All patients enrolled in the study had systolic dysfunction (LV ejection fraction <50%) without significant coronary artery stenosis, as assessed by coronary angiography. Written informed consent was obtained from all patients prior to their inclusion in the study. The study protocol was approved by the committee overseeing clinical and genetics research at our institution and was performed in accordance with the Declaration of Helsinki.

Figure 1 Flow chart of the study cohort.
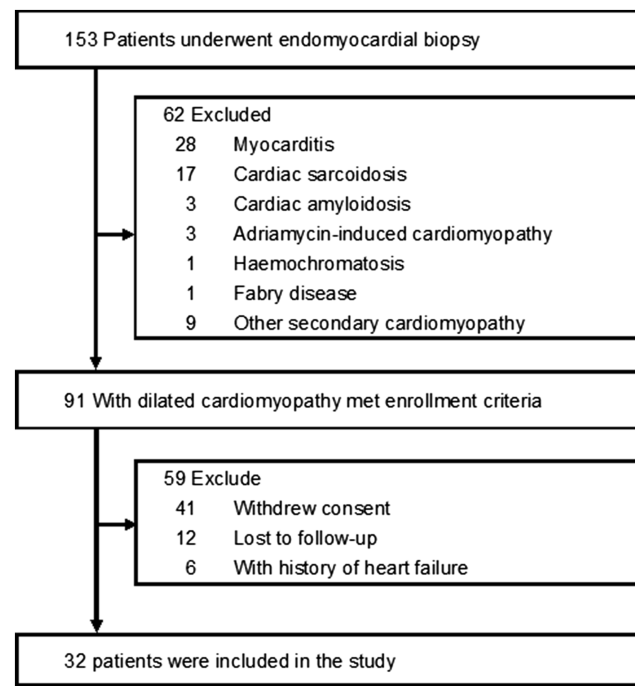
Clinical data collection, including endomyocardial biopsy

On admission, all patients underwent routine laboratory analyses and trans-thoracic echocardiography. Two-dimensional, M-mode, and colour Doppler imaging was performed according to the standardized methods of the American Society of Echocardiography.[12] Cardiac catheterization was performed together with EMB and performed under radiographic guidance with continuous electrocardiographic monitoring. Tissue samples were collected from the LV infero-posterior wall using a 7 Fr bioptome (Cordis; Johnson & Johnson Co, New Brunswick, NJ) by retrograde approach.

Tissue preparation

Preparation of biopsy specimens for light and electron microscopic analyses has been described previously.[7,9] Ultrastructural variables such as myofilament changes were classified as positive (when identified in the cytoplasm of cardiomyocytes) or negative.[7] Photomicrographs of 200 cardiomyocytes were evaluated per patient. Three of the authors evaluated all electron microscopy results for EMB samples (T. S., A. A., and Y. S.), with each sample examined three times in random order; these examiners were blinded to the clinical background and results of genetic testing of the patients. Any discrepancies in the ultrastructural evaluations were decided by consensus. The Z-line is a structure

with high electron density to which myofilament is bound. Abnormal Z-line was defined as a structure that has the same density as normal Z-line and can adhere to one or several myofilaments, even if myofilament lysis occurs. The M-line is in the centre of the sarcomere between the Z-lines. Obscured M-line was defined as obscured and discontinuous in nature.

DNA isolation

Genomic DNA was extracted from peripheral blood lymphocytes using Genomix Kit (Biologica Co., Nagoya, Japan) following the manufacturer's protocol.

Whole-exome sequencing

Whole-exome sequencing was performed by Riken Genesis Co., Ltd. in Japan. Exon capture was performed using the SureSelect[XT] Human All Exon V6 Kit (Agilent Technologies, Santa Clara, CA), and sequencing was performed on the Illumina HiSeq 2500 platform (Illumina Inc, San Diego, CA). Sequence mapping was performed using the Burrows-Wheeler Aligner 0.7.10. Mapping results were corrected using Picard (Ver. 1.73) for removing duplicates and Genome Analysis Toolkit (GATK Ver. 1.6-13) for local alignment and quality score recalibration. Variant detection was performed with multi-sample calling with GATK.

Variant filtering and pathogenicity assessment

Variant annotation was performed using software developed in-house by Riken Genesis Co., Ltd. A series of filters were used to prioritize variants. Variants were given higher priority when (i) they had a high-quality score to coordinates with variant quality score recalibration passing and variant call quality score $\geq$30, (ii) they were non-synonymous variants (i.e. missense, nonsense, frameshift insertion/deletion, in-frame insertion/deletion, or splice error), and (iii) less common in reference databases [minor allele frequency (MAF) $\leq$0.0005 within genomAD in any ethnic group (n = 125 748, https://gnomad.broadinstitute.org/) or East Asian population group (n = 9197, https://gnomad.broadinstitute.org/), 1000 Genome Project (n = 2504, https://www.internationalgenome.org/1000-genomes-browsers), the National Heart, Lung, and Blood Institute Grand Opportunity Exome Sequencing Project (n = 6503), and Human Genetic Variation Database (n = 3248, http://www.hgvd.genome.med.kyoto-u.ac.jp/) databases]. The MAF was calculated to be 0.0004 using an estimated maximum prevalence of 1:250[13] and was set to $\leq$0.0005 cut-off. Variants meeting these criteria underwent a further gene-specific surveillance for all known 75 cardiomyopathy-susceptibility and 41 arrhythmia-susceptibility genes (N = 116; *Table 1*). The American College of Medical Genetics guidelines modified specifically for DCM[14] for the interpretation of sequence variants were used to classify identified variants as pathogenic (P), likely pathogenic (LP), or variant of uncertain significance (VUS).

Those gene variants were confirmed using standard polymerase chain reaction and Sanger sequencing methods.

Statistical analysis

Continuous variables were expressed as median values reported with 25th and 75th percentiles. Variables were evaluated by one-way analysis of variance in the case of normally distributed data and by the Kruskal–Wallis test if data were not normally distributed, as determined by the Shapiro–Wilk test. The distribution of myofilament lysis in cardiomyocytes was evaluated by χ^2 or Fisher's exact test. Statistical analyses were performed using the SPSS software package (SPSS Inc., Chicago, IL), and $P < 0.05$ was considered significant.

Results

Patient characteristics

The clinical, genetic, histopathological, and ultrastructural characteristics of the patients are summarized in *Tables 2* and *3*. During the follow-up period [7.6 (3.9–8.0) years], 12 patients (38%) were readmitted because of HF recurrence, one patient (P7, *Table 4*) received HTx, and four patients (13%) died. One death was from multiple organ failure due to decompensated HF with inability to control ventricular arrhythmia (P1, *Table 4*), and three were due to sudden cardiac death (P9 in *Table 4* and P20 and P26 in *Table 5*).

American College of Medical Genetics classifications of variants

In 32 patients, a total of 404 variants were detected (*Table 1*). After filtering with MAF and the American College of Medical Genetics guidelines, 62 ultrarare variants remained, including 5 P and 10 LP variants in 14 patients (44% of 32, *Table 4*) and 35 VUSs in 24 patients (75% of 32, *Table 5*). VUS included two variants (6% of 35, *Table 5*) that could be upgraded to LP variants if there was additional evidence supporting pathogenicity, and six variants (17% of 35, *Table 5*) that could be downgraded to likely benign variants if there was additional evidence supporting benign impact.

Table 1 List of 116 genes with previous evidence of association with cardiomyopathy and arrhythmia

	Gene symbol	NCBI RefSeq	Protein name	Location	*N*
Cardiomyopathy-susceptibility genes					
1	ACTC1	NM_005159.5	Actin, alpha, cardiac muscle 1	15q14	0
2	ACTN2	NM_001103.3	Actinin alpha 2	1q43	2
3	APLN	NM_017413.5	Apelin	Xq26.1	1
4	BAG3	NM_004281.3	BAG cochaperone 3	10q26.11	4
5	CACNA2D1	NM_000722.4	Calcium voltage-gated channel auxiliary subunit alpha2delta 1	7q21.11	1
6	CALR3	NM_145046.5	Calreticulin 3	19p13.11	2
7	CAMK2D	NM_001221.4	Calcium/calmodulin-dependent protein kinase II delta	4q26	1
8	CAV3	NM_033337.3	Caveolin 3	3p25.3	2
9	CCN2	NM_001901.3	Cellular communication network factor 2	6q23.2	0
10	COX15	NM_078470.6	COX15, cytochrome *c* oxidase assembly homologue	10q24.2	4
11	CRYAB	NM_001289807.1	Crystallin alpha B	11q23.1	2
12	CSRP3	NM_003476.5	Cysteine-rich and glycine-rich protein 3	11p15.1	0
13	CTF1	NM_001330.3	Cardiotrophin 1	16p11.2	0
14	DES	NM_001927.4	Desmin	2q35	1
15	DLG1	NM_004087.2	Discs large MAGUK scaffold protein 1	3q29	1
16	DMD	NM_004006.2	Dystrophin	Xp21.2-p21.1	19
17	DNM1L	NM_012062.5	Dynamin 1 like	12p11.21	1
18	DSC2	NM_004949.5	Desmocollin 2	18q12.1	1
19	DSG2	NM_001943.5	Desmoglein 2	18q12.1	2
20	DSP	NM_004415.4	Desmoplakin	6p24.3	12
21	DTNA	NM_001390.4	Dystrobrevin alpha	18q12.1	2
22	EMD	NM_000117.3	Emerin	Xq28	0
23	EYA4	NM_004100.5	EYA transcriptional coactivator and phosphatase 4	6q23.2	1
24	FGF12	NM_021032.4	Fibroblast growth factor 12	3q28-q29	0
25	FHL2	NM_001039492.3	Four and a half LIM domains 2	2q12.2	3
26	FKTN	NM_006731.2	Fukutin	9q31.2	1
27	GAA	NM_000152.5	Glucosidase alpha, acid	17q25.3	8
28	GATA5	NM_080473.5	GATA-binding protein 5	20q13.33	1
29	GATA6	NM_005257.5	GATA-binding protein 6	18q11.2	1
30	GATAD1	NM_021167.5	GATA zinc finger domain-containing 1	7q21.2	1
31	GLA	NM_000169.3	Galactosidase alpha	Xq22.1	0
32	HEY2	NM_012259.3	Hes related family bHLH transcription factor with YRPW motif 2	6q22.31	0
33	JPH2	NM_020433.5	Junctophilin 2	20q13.12	1
34	JUP	NM_001352773.1	Junction plakoglobin	17q21.2	1
35	LAMA4	NM_001105206.3	Laminin subunit alpha 4	6q21	11
36	LAMP2	NM_001122606.1	Lysosomal-associated membrane protein 2	Xq24	0
37	LDB3	NM_001080114.2	LIM domain binding 3	10q23.2	5
38	LMNA	NM_170707.4	Lamin A/C	1q22	3
39	MLIP	NM_138569.2	Muscular LMNA interacting protein	6p12.1	12
40	MYBPC3	NM_000256.3	Myosin-binding protein C, cardiac	11p11.2	5
41	MYH6	NM_002471.3	Myosin heavy chain 6	14q11.2	5
42	MYH7	NM_000257.4	Myosin heavy chain 7	14q11.2	3
43	MYL2	NM_000432.4	Myosin light chain 2	12q24.11	0
44	MYL3	NM_000258.3	Myosin light chain 3	3p21.31	1
45	MYLK2	NM_033118.4	Myosin light chain kinase 2	20q11.21	1
46	MYLK3	NM_182493.3	Myosin light chain kinase 3	16q11.2	3
47	MYOZ2	NM_016599.5	Myozenin 2	4q26	0
48	MYPN	NM_032578.3	Myopalladin	10q21.3	6
49	NEBL	NM_006393.2	Nebulette	10p12.31	9
50	NEXN	NM_144573.3	Nexilin F-actin binding protein	1p31.1	2
51	PKP2	NM_004572.3	Plakophilin 2	12p11.21	1
52	PLN	NM_002667.5	Phospholamban	6q22.31	0
53	PRKAG2	NM_016203.4	Protein kinase AMP-activated non-catalytic subunit gamma 2	7q36.1	4
54	PSEN1	NM_000021.4	Presenilin 1	14q24.2	0
55	PSEN2	NM_000447.3	Presenilin 2	1q42.13	2
56	RBM20	NM_001134363.3	RNA-binding motif protein 20	10q25.2	8
57	RYR2	NM_001035.3	Ryanodine receptor 2	1q43	4
58	SCO2	NM_005138.3	SCO2, cytochrome *c* oxidase assembly protein	22q13.33	1
59	SDHA	NM_004168.4	Succinate dehydrogenase complex flavoprotein subunit A	5p15.33	4
60	SGCD	NM_000337.5	Sarcoglycan delta	5q33.2-q33.3	0
61	SLC25A4	NM_001151.4	Solute carrier family 25 member 4	4q35.1	1
62	TBX20	NM_020417.1	T-box transcription factor 20	7p14.2	1

(Continues)

Table 1 (continued)

	Gene symbol	NCBI RefSeq	Protein name	Location	N
63	TBX5	NM_080717.3	T-box transcription factor 5	12q24.21	2
64	TCAP	NM_003673.4	Titin-cap	17q12	0
65	TGFB3	NM_003239.4	Transforming growth factor beta 3	14q24	0
66	TMEM43	NM_024334.3	Transmembrane protein 43	3p25.1	7
67	TMPO	NM_003276.2	Thymopoietin	12q23.1	2
68	TNNC1	NM_003280.3	Troponin C1, slow skeletal and cardiac type	3p21.1	0
69	TNNI3	NM_000363.5	Troponin I3, cardiac type	19q13.4	2
70	TNNT2	NM_000364.4	Troponin T2, cardiac type	1q32.1	4
71	TP63	NM_003722.5	Tumour protein p63	3q28	0
72	TPM1	NM_001018004.2	Tropomyosin 1 (alpha)	15q22.2	2
73	TTN	NM_133378.4	Titin	2q31.2	142
74	TTR	NM_000371.3	Transthyretin	18q12.1	0
75	VCL	NM_003373.4	Vinculin	10q22.2	2
Arrhythmia-susceptibility genes					
1	ABCC8	NM_000352.6	ATP-binding cassette subfamily C member 8	11p15.1	0
2	ABCC9	NM_005691.3	ATP-binding cassette subfamily C member 9	12p12.1	0
3	AKAP9	NM_005751.4	A-kinase anchor protein 9	7q21.2	16
4	ANK2	NM_001148.6	Ankyrin 2	4q25-q26	5
5	ANKRD1	NM_014391.2	Ankyrin repeat domain 1	10q23.31	0
6	CACNA1C	NM_000719.7	Calcium voltage-gated channel subunit alpha1 C	12p13.33	4
7	CACNB2	NM_000724.4	Calcium voltage-gated channel auxiliary subunit beta 2	10p12	0
8	CALM1	NM_001363669.1	Calmodulin 1	14q32.11	0
9	CASQ2	NM_001232.3	Calsequestrin 2	1p13.1	3
10	DPP6	NM_130797.4	Dipeptidyl peptidase like 6	7q36.2	1
11	GJA1	NM_000165.5	Gap junction protein alpha 1	6q22.31	0
12	GJA5	NM_181703.4	Gap junction protein alpha 5	1q21.2	0
13	GJD4	NM_153368.3	Gap junction protein delta 4	10p11.21	2
14	GPD1L	NM_015141.4	Glycerol-3-phosphate dehydrogenase 1 like	3p22.3	0
15	HCN4	NM_005477.3	Hyperpolarization-activated cyclic nucleotide-gated potassium channel 4	15q24.1	1
16	KCNA5	NM_002234.4	Potassium voltage-gated channel subfamily A member 5	12p13.32	1
17	KCND3	NM_172198.2	Potassium voltage-gated channel subfamily D member 3	1p13.2	0
18	KCNE1	NM_000219.6	Potassium voltage-gated channel subfamily E regulatory subunit 1	21q22.12	1
19	KCNE2	NM_172201.1	Potassium voltage-gated channel subfamily E regulatory subunit 2	21q22.11	0
20	KCNE3	NM_005472.4	Potassium voltage-gated channel subfamily E regulatory subunit 3	11q13.4	0
21	KCNE5	NM_012282.4	Potassium voltage-gated channel subfamily E regulatory subunit 5	Xq23	0
22	KCNH2	NM_000238.4	Potassium voltage-gated channel subfamily H member 2	7q36.1	2
23	KCNJ2	NM_000891.3	Potassium inwardly rectifying channel subfamily J member 2	17q24.3	0
24	KCNJ5	NM_000890.5	Potassium inwardly rectifying channel subfamily J member 5	11q24.3	1
25	KCNJ8	NM_004982.4	Potassium inwardly rectifying channel subfamily J member 8	12p12.1	0
26	KCNQ1	NM_000218.3	Potassium voltage-gated channel subfamily Q member 1	11p15.5-p15.4	2
27	NKX2-5	NM_001166175.2	NK2 homeobox 5	5q34	0
28	NOS1AP	NM_014697.3	Nitric oxide synthase 1 adaptor protein	1q23.3	1
29	RANGRF	NM_016492.5	RAN guanine nucleotide release factor	17p13	0
30	SCN10A	NM_006514.3	Sodium voltage-gated channel alpha subunit 10	3p22.2	10
31	SCN1B	NM_001037.5	Sodium voltage-gated channel beta subunit 1	19q13.11	4
32	SCN2B	NM_004588.5	Sodium voltage-gated channel beta subunit 2	11q23.3	0
33	SCN3B	NM_018400.3	Sodium voltage-gated channel beta subunit 3	11q24.1	0
34	SCN4B	NM_001142348.2	Sodium voltage-gated channel beta subunit 4	11q23.3	1
35	SCN5A	NM_198056.2	Sodium voltage-gated channel alpha subunit 5	3p22.2	5
36	SLMAP	NM_007159.4	Sarcolemma associated protein	3p14.3	0
37	SNTA1	NM_003098.3	Syntrophin alpha 1	20q11.21	1
38	TAZ	NM_000116.5	Tafazzin	Xq28	0
39	TRDN	NM_001251987.2	Triadin	6q22.31	9
40	TRPM4	NM_017636.4	Transient receptor potential cation channel subfamily M member 4	19q13.33	2
41	TRPM7	NM_017672.6	Transient receptor potential cation channel subfamily M member 7	15q21.2	1

Table 2 Patient characteristics

	All patients (N = 32)	No myofilament changes (N = 3)	Focal derangement of myofilaments (N = 17)	Diffuse myofilament lysis (N = 12)	P-value
Clinical characteristics					
Age (years)	51.0 (40.0–64.0)	50.6 ± 13.4	58.0 (41.0–67.0)	51.7 ± 12.0	0.781
Male	24 (75%)	3 (60%)	9 (60%)	12 (100%)	0.039
Systolic blood pressure (mmHg)	132.0 (115.5–157.3)	132.0 (132.0–150.0)	135.3 ± 31.2	133.6 ± 25.0	0.529
Diastolic blood pressure (mmHg)	79.0 (69.0–97.3)	88.8 ± 33.8	78.0 (66.0–94.0)	86.8 ± 24.3	0.966
Heart rate (b.p.m.)	91.8 ± 24.3	82.0 ± 17.9	95.6 ± 27.2	91.0 ± 23.1	0.565
NYHA Scale III and IV	15 (47%)	2 (40%)	8 (53%)	5 (42%)	0.804
Co-morbidities					
Atrial fibrillation	14 (44%)	1 (20%)	7 (47%)	6 (50%)	0.526
Hypertension	19 (59%)	3 (60%)	9 (60%)	7 (58%)	0.996
Diabetes	13 (41%)	4 (80%)	5 (33%)	4 (33%)	0.159
Renal dysfunction[a]	6 (19%)	1 (20%)	2 (13%)	3 (25%)	0.759
Clinical chemistry					
B-type natriuretic peptide (pg/mL)	561.4 (341.2–1407.7)	880.7 ± 524.7	420.1 (262.7–649.3)	1185.4 ± 1077.0	0.335
C-reactive protein (mg/dL)	0.3 (0.1–0.9)	0.5 (0.2–0.9)	0.2 (0.1–0.4)	0.7 ± 0.6	0.091
Haemoglobin (g/dL)	14.2 ± 2.2	15.2 ± 3.1	13.4 ± 2.4	14.8 ± 1.2	0.150
Total bilirubin (mg/dL)	0.9 (0.7–1.1)	1.4 ± 1.3	0.8 ± 0.3	1.0 (0.6–1.2)	0.121
Echocardiographic data					
Left atrial dimension (mm)	46.4 ± 7.2	44.0 ± 8.3	44.7 ± 6.0	49.7 ± 7.7	0.146
Left ventricular ejection fraction (%)	31.7 ± 10.1	45.0 (17.0–45.0)	33.5 ± 9.9	26.5 (19.0–31.3)	0.577
Left ventricular diastolic dimension (mm)	62.5 ± 8.2	58.4 ± 6.4	61.3 ± 9.6	65.8 ± 6.2	0.181
Left ventricular systolic dimension (mm)	52.8 ± 9.6	47.6 ± 11.6	51.4 ± 10.5	56.8 ± 6.2	0.144
Interventricular septum thickness (mm)	10.1 ± 2.0	10.0 ± 2.7	9.9 ± 1.7	10.4 ± 2.1	0.775
Posterior wall thickness (mm)	9.0 (7.0–10.0)	9.4 ± 2.3	9.0 (7.0–10.0)	10.1 ± 3.0	0.314
Left ventricular reverse remodelling	15 (47%)	4 (80%)	5 (33%)	6 (50%)	0.201
Outcome of morphometry					
Cellular diameter (μm)	18.2 ± 1.6	18.1 ± 0.6	17.7 ± 1.7	19.3 (15.6–19.9)	0.201
Nuclear diameter (μm)	8.2 ± 0.8	8.3 ± 0.3	8.2 ± 0.8	8.2 ± 0.9	0.983
Proportion of fibrosis (%)	12.9 ± 7.7	15.7 ± 6.9	10.1 ± 5.4	15.4 ± 9.5	0.163
Genetic analysis					
Pathogenic/likely pathogenic variants	14 (44%)	0 (0%)	7 (41%)	7 (58%)	0.052
Sarcomeric gene variants[b]	5 (16%)	0 (0%)	4 (24%)	1 (8%)	0.320
Non-sarcomeric gene variants	11 (34%)	0 (0%)	3 (20%)	8 (58%)	0.035
Nuclear gene variant[c]	3 (9%)	0 (0%)	0 (0%)	3 (25%)	0.077
Gap junction gene variant[d]	2 (6%)	0 (0%)	0 (0%)	2 (17%)	0.200
Channel gene variant[e]	3 (13%)	0 (0%)	2 (20%)	1 (8%)	0.182
Follow-up data					
Amiodarone	5 (16%)	0 (0%)	3 (20%)	2 (17%)	0.587
ICD or CRT-D implantation	4 (13%)	1 (20%)	2 (13%)	2 (17%)	0.937
Ventricular tachyarrhythmia	6 (19%)	0 (0%)	2 (13%)	4 (33%)	0.226
Heart failure recurrence	12 (38%)	1 (20%)	6 (40%)	5 (42%)	0.698
Heart transplantation	1 (3%)	0 (0%)	1 (7%)	0 (0%)	0.583
Mortality	4 (13%)	0 (0%)	1 (7%)	3 (25%)	0.435
Mean follow-up duration (years)	7.6 (3.9–8.0)	7.6 ± 1.7	7.9 (3.6–8.4)	7.5 (0.4–7.9)	0.414

CRT-D, cardiac resynchronization therapy defibrillator; ICD, implantable cardioverter defibrillator; NYHA, New York Heart Association.
Data are given as median values (inter-quartile range, 25th and 75th percentiles) or number of patients, with percentages in parentheses, as appropriate.
[a]Renal dysfunction was classified as glomerular filtration rate <60 mL/min/1.73 m^2.
[b]Sarcomeric genes were *MYBP3* and *TTN*.
[c]Nuclear gene was *TMEM43*.
[d]Gap junction gene was *DSP*.
[e]Channel gene was *TRPM4*.

Ultrastructural features of cardiomyocytes and gene variants

Pathogenic or LP variants involved five sarcomeric gene variants in five patients (16% of 32): an *MYBPC3* variant and four *TTN* variants. Electron microscopy revealed distinctive types of focal derangement of myofilaments (sarcomere damage) depending on the genes. Compared with normal cardiomyocytes (*Figure 2A*), a patient with a *MYBPC3* variant (c.2833_2834delCG; P1, *Table 4*) showed disorganized

Table 3 Characteristics of patients with gene variants of unknown significance or no variant

	All patients (N = 18)	No myofilament changes (N = 3)	Focal derangement of myofilaments (N = 10)	Diffuse myofilament lysis (N = 5)	P-value
Clinical characteristics					
Age (years)	50.0 (40.0–64.8)	40.5 (40.3–40.8)	62.0 (39.5–67.0)	56.0 (40.0–62.0)	0.998
Male	15 (83%)	3 (100%)	7 (70%)	5 (100%)	0.237
Systolic blood pressure (mmHg)	133.0 (117.5–155.3)	141.0 (136.5–145.5)	130.0 (119.0–140.0)	157.0 (102.0–162.0)	0.952
Diastolic blood pressure (mmHg)	78.0 (66.0–108.5)	84.0 (81.0–87.0)	74.0 (66.0–94.0)	112.0 (62.0–117.0)	0.963
Heart rate (b.p.m.)	86.5 (74.5–98.8)	79.0 (73.5–84.5)	88.0 (77.0–97.5)	85.0 (54.0–112.0)	0.775
NYHA Scale III and IV	8 (44%)	1 (33%)	5 (50%)	2 (40%)	0.854
Co-morbidities					
Atrial fibrillation	5 (38%)	1 (33%)	3 (30%)	1 (20%)	0.895
Hypertension	11 (61%)	1 (33%)	7 (70%)	3 (60%)	0.520
Diabetes	6 (33%)	1 (33%)	4 (40%)	1 (20%)	0.741
Renal dysfunction	4 (22%)	1 (33%)	2 (20%)	1 (20%)	0.879
Clinical chemistry					
B-type natriuretic peptide (pg/mL)	435.1 (262.1–828.6)	1114.9 (972.9–1256.8)	329.5 (260.9–539.0)	821.7 (434.5–1470.0)	0.092
C-reactive protein (mg/dL)	0.2 (0.1–0.7)	0.1 (0.1–0.2)	0.1 (0.1–0.3)	0.9 (0.9–0.9)	0.058
Haemoglobin (g/dL)	14.5 (13.4–16.3)	18.3 (18.1–18.6)	14.3 (12.8–15.4)	13.9 (13.7–15.7)	0.087
Total bilirubin (mg/dL)	0.9 (0.7–1.1)	1.2 (1.0–1.5)	0.9 (0.5–1.1)	1.0 (0.9–1.3)	0.339
Echocardiographic data					
Left atrial dimension (mm)	45.0 (42.0–50.8)	46.6 (44.3–48.8)	45.0 (43.5–50.0)	45.0 (42.0–51.0)	0.551
Left ventricular ejection fraction (%)	29.0 (21.5–41.0)	31.0 (24.0–38.0)	33.0 (23.5–39.0)	25.0 (21.0–26.0)	0.834
Left ventricular diastolic dimension (mm)	63.5 (62.0–70.0)	60.0 (58.0–62.0)	64.0 (60.0–71.0)	62.0 (62.0–67.0)	0.979
Left ventricular systolic dimension (mm)	54.5 (48.3–59.8)	50.5 (46.8–54.3)	54.0 (48.5–61.0)	55.0 (54.0–60.0)	0.834
Interventricular septum thickness (mm)	10.0 (9.0–11.0)	9.0 (8.0–10.0)	10.0 (9.5–11.0)	10.0 (9.0–10.0)	0.656
Posterior wall thickness (mm)	9.5 (7.3–10.0)	10.0 (8.5–11.5)	10.0 (7.5–10.0)	9.0 (8.0–13.0)	0.868
Left ventricular reverse remodelling	13 (72%)	3 (100%)	6 (60%)	4 (80%)	0.487
Outcome of morphometry					
Cellular diameter (μm)	18.4 (17.1, 19.5)	18.5 (18.3, 18.6)	17.4 (17.0–18.9)	19.8 (19.1–20.0)	0.277
Nuclear diameter (μm)	8.3 (8.0, 9.0)	8.2 (8.1, 8.3)	8.3 (7.7–8.5)	9.1 (8.1–9.3)	0.509
Proportion of fibrosis (%)	10.3 (7.4, 18.3)	13.2 (10.3, 16.0)	10.0 (7.1–11.3)	25.0 (12.3–30.3)	0.147
Genetic analysis					
Sarcomeric gene variants[a]	4 (22%)	0 (0%)	2 (20%)	2 (40%)	0.407
Non-sarcomeric gene variants	10 (56%)	1 (33%)	5 (50%)	4 (80%)	0.380
Nuclear gene variant[b]	1 (6%)	0 (0%)	0 (0%)	1 (20%)	0.252
Gap junction gene variant[c]	3 (17%)	1 (33%)	1 (10%)	1 (20%)	0.619
Channel gene variant[d]	4 (22%)	0 (0%)	2 (20%)	2 (40%)	0.407
Follow-up data					
Amiodarone	1 (6%)	0 (0%)	1 (10%)	0 (0%)	0.655
ICD or CRT-D implantation	2 (11%)	0 (0%)	1 (10%)	1 (20%)	0.675
Ventricular tachyarrhythmia	4 (22%)	0 (0%)	2 (20%)	2 (40%)	0.407
Heart failure recurrence	4 (22%)	0 (0%)	2 (20%)	2 (40%)	0.407
Heart transplantation	0 (0%)	0 (0%)	0 (0%)	0 (0%)	—
Mortality	2 (11%)	0 (0%)	1 (10%)	1 (20%)	0.675
Mean follow-up duration (years)	8.0 (7.7–8.7)	8.1 (7.9–8.4)	8.1 (7.9–8.9)	7.9 (7.5–7.9)	0.461

Abbreviations as in *Table 2*.
[a]Sarcomeric genes were *NEXN, SNTA1, TTN, DMD, MYLK3,* and *MLIP.*
[b]Nuclear gene was *LMNA.*
[c]Gap junction genes were *DUP, PKP2,* and *GJD4.*
[d]Channel genes were *SCN4B, SLC25A4, KCNA4,* and *KCNH2.*

Table 4 Patients' summary and evaluation with pathogenic or likely pathogenic gene variants

Case	Age (years), sex	Ultrastructural findings	Genes	Variant	Amino acid	ACMG criteria met	ACMG classification
Sarcomeric gene variants							
P1	36, male	Focal derangement	MYBPC3	c.2833_2834delCG	p.R945fs	PS1, PM2	Likely pathogenic
P2	42, female	Focal derangement	TTN	c.7111T>A	p.Y23704*	PVS1_St, PM2	Likely pathogenic
P3	51, female	Focal derangement	TTN	c.79276delA	p.R26426fs	PVS1_St, PM2	Likely pathogenic
P4	62, male	Diffuse myofilament lysis	TTN	c.72233delT	p.I24078fs	PSV1_St, PM2	Likely pathogenic
			DSP	c.4996C>T	p.R1666W	PS1, PM2	Likely pathogenic
P5	48, female	Focal derangement	TTN	c.14488_14491delCAGT	p.Q4830fs	PS1, PM2	Likely pathogenic
Nuclear membranous gene variants							
P6	38, male	Diffuse myofilament lysis	TMEM43	c.271A>G	p.I91V	PS4, PP1_St	Pathogenic
P7	47, female	Diffuse myofilament lysis	TMEM43	c.271A>G	p.I91V	PS4, PP1_St	Pathogenic
P8	58, male	Diffuse myofilament lysis	TMEM43	c.271A>G	p.I91V	PS4, PP1_St	Pathogenic
Gap junction gene variants							
P9	64, male	Diffuse myofilament lysis	DSP	c.5589_5590delCC	p.D1863fs	PVS1_M, PM2, PM4	Likely pathogenic
Ion channel gene variants							
P10	58, male	Focal derangement	TRPM4	c.1532T>A	p.L511Q	PS4, PP1, PP3	Likely pathogenic
P11	44, male	Diffuse myofilament lysis	TRPM4	c.1532T>A	p.L511Q	PS4, PP1, PP3	Likely pathogenic
P12	73, male	Focal derangement	TRPM4	c.1532T>A	p.L511Q	PS4, PP1, PP3	Likely pathogenic
Developmental gene variants							
P13	73, female	Focal derangement	TBX5	c.52C>G	p.D18H	PS1, PS4, PP1	Pathogenic
P14	50, male	Diffuse myofilament lysis	TBX5	c.52G>C	p.D18H	PS1, PS4, PP1	Pathogenic

ACMG, American College of Medical Genetics.

myofilaments with residual but abnormal Z-line structure (*Figure 2B*). Patients with *TTN* variants had ultrastructural alterations compatible with the location of the titin domain where their mutated nucleotide sequences were located. P2 had a nonsense variant, and P3 and P4 hosted frameshift variants. All variants were in exon 325 that encodes the A-band domain.[15] Ultrastructural analysis showed obscured M-line and sparse myofilaments (*Figure 2C* and 2*D*). P5 had a *TTN* frameshift variant (c.14488_14491delCAGT), which was in Exon 45, the I-band domain.[15] Ultrastructural analysis showed sparse myofilaments with mitochondrial infiltrates and glycogen granules. The patient also had focal areas of disrupted sarcomere structure with lipid droplets (*Figure 2E* and 2*F*); this region had fewer glycogen granules and mitochondria than the surrounding areas, while the boundary was unclear. In five patients with sarcomeric gene variants, diffuse myofilament lysis was not found except in one case (P4), who also had a *DSP* variant.

Three patients had the same *TMEM43* variant (c.271A>G). One had tiny nuclear changes with diffuse myofilament lysis expanded around the nuclei (P6, *Table 4*). The other two patients (P7 and P8), both with personal histories of potentially fatal ventricular tachyarrhythmia, had extensive diffuse myofilament lysis surrounding nuclei with lipofuscin deposition (*Figure 2G*). Diffuse myofilament lysis was observed in the perinuclear area of cardiomyocytes in all three cases (perinuclear vs. peripheral was 100% vs. 9%; *P* = 0.011).

Two patients with *DSP* variants (P4 and P9, *Table 4*) showed diffuse myofilament lysis spreading to the peripheral areas of cardiomyocytes (perinuclear vs. peripheral was 8% vs. 100%; *P* = 0.033), occurring at both sides of intercalated disc structures containing desmosome-derived elements with high electron density (*Figure 2D*).

There were three patients with same *TRPM4* variant (c.1532T>A) and two patients with same *TBX5* variant (c.52G>C); however, it was difficult to determine whether there were specific changes based on ultrastructural examination.

Case series with clinical implications

Some patients might have been treated earlier and more effectively if their causal variants in DCM genes were identified. A 36-year-old man (P1, *Table 4*) hosted a frameshift variant in *MYBPC3* (c.2833_2834delCG), classified as LP. Despite optimal therapy, he developed HF due to sustained ventricular tachycardia, and insertion of an implantable cardioverter defibrillator was performed. After HF recurrence, implantable cardioverter defibrillator treatment was changed to cardiac resynchronization therapy defibrillator treatment. Seven years from the first hospitalization, his ventricular arrhythmia could not be controlled, and he died from multiple organ failure due to severe HF. While considering HTx, his condition

Table 5 Patients' summary with variants of unknown significance

Case	Age, sex	Ultrastructural findings	Genes	Mutation	Protein	ACMG criteria met
Additional gene variants of unknown significance in patients with pathogenic or likely pathogenic variants						
P1	36, male	Focal derangement	MYH6	c.5661G>A	p.A1887_splice	PM2
P2	42, female	Focal derangement	FHL2	c.191A>G	p.E64G	PM2
P3	51, female	Focal derangement	SCN5A	c.2497G>A	p.G833R	PS1
P5	48, female	Focal derangement	RYR2	c.3423+3G>A	p.T1142_splice	PM2
P7	47, female	Diffuse myofilament lysis	DMD	c.4859A>G	p.E1620G	PM2, PP3
			TRPM4	c.3304T>G	p.S1102A	PS4, BP4[b]
P8	58, male	Diffuse myofilament lysis	LAMA4	c.4494delT	p.R1498fs	PM2, PM4[a]
			SCN10A	c.4205T>C	p.I1402T	PP3
P9	64, male	Diffuse myofilament lysis	RBM20	c.3067G>T	p.D1023Y	PM2, PP3
P10	58, male	Focal derangement	TPM1	c.2T>C	p.M1T	PM2, PP3
P11	44, male	Diffuse myofilament lysis	MLIP	c.1309C>T	p.P437S	PM2
P12	73, male	Focal derangement	TBX20	c.374C>T	p.S125L	PP3
			HCN4	c.2827C>T	p.P943S	PM2, BP4[b]
P14	50, male	Diffuse myofilament lysis	PSEN2	c.1262C>T	p.T421M	PP3
Sarcomeric gene variants						
P15	62, male	Focal derangement	NEXN	c.919C>A	p.P307T	PP3
P16	39, male	Diffuse myofilament lysis	SNTA1	c.1432G>C	p.D478H	PM2, PP3
P17	62, male	Diffuse myofilament lysis	TTN	c.37202-2G>T	p.D12401_splice	PM2
			SLC25A4	c.628A>G	p.I210V	PM2
			DMD	c.2404A>C	p.K802Q	PM2, BP5[b]
			GJD4	c.932G>A	p.R311Q	PM2, BP4[b]
P18	69, female	Focal derangement	MYLK3	c.844C>G	p.P282A	BP4[b]
			DES	c.976C>T	c.976C>T	PM2, PP3
			MLIP	c.2608C>T	p.R870C	PM2, PP3
Nuclear membranous gene variants						
P19	56, male	Diffuse myofilament lysis	LMNA	c.1123G>A	p.A375T	PM2, PP3
			RYR2	c.2300C>G	p.S767W	PM2, PP3
Gap junction gene variants						
P20	35, male	Focal derangement	JUP	c.1907G>A	p.S636F	PM2, PP3
P21	41, male	—	PKP2	c.592G>A	p.E198K	PM2, PP3
Ion channel gene variants						
P22	40, male	Diffuse myofilament lysis	SCN4B	c.463+3A>T	p.V155_splice	PM2
P23	64, female	Focal derangement	KCNA5	c.1103_1110delACTTCATC	p.Y368fs	PM2, PM4[a]
			DTNA	c.2095C>T	p.R699C	PM2, PP3
P24	39, male	Focal derangement	KCNH2	c.28C>T	p.P10S	PM2, PP3
			TBX5	c.1034C>T	p.S345F	PM2
Developmental gene variants						
P25	71, male	Diffuse myofilament lysis	RBM20	c.1552C>T	p.R518C	PM2, PP3
Others						
P26	44, male	Focal derangement	OXTR	c.1126C>T	p.R376C	PS1
P27	70, male	Focal derangement	CALR3	c.28G>A	p.A10T	PM2, BP4[b]

ACMG, American College of Medical Genetics.
[a]Can be upgraded to likely pathogenic variants if they have other evidence supporting pathogenicity.
[b]Can be upgraded to likely benign variants if they have other evidence supporting benign impact.

worsened and HTx was not implemented. Ultrastructural findings of EMB at his initial admission were not so severe, with only sarcomeric changes (*Figure 2B*). EMB was re-examined because of concern of acute myocarditis when his HF became uncontrollable immediately before his death. Acute myocarditis was negative histologically, but severe findings were observed by electron microscopy, especially diffuse myofilament lysis and lobulated nuclei with highly condensed chromatin (*Figure 3A*).

A 47-year-old woman (P7, *Table 4*) hosted a *TMEM43* variant (c.271A>G) designated as LP. She had chest pain at admission due to HF, and the acetylcholine load test provoked coronary artery spasm. As atrial fibrillation was also observed, myocardial ischaemia and arrhythmia were thought to be the cause of HF. Beta-blockers were avoided to prevent

exacerbating coronary spasms. After 13 months, severe decompensated HF recurred. After repeated HF attacks, she received an HTx 5 years after the onset of HF. Ultrastructural findings of EMB at her initial admission with HF showed diffuse myofilament lysis; areas where myofilaments were replaced with mitochondrial hyperplasia. Mitochondrial abnormality (*Figure 3B*) and mitophagy, as activated selective autophagy (*Figure 3C*), were also found.

Discussion

The present study compared the results of whole-exome sequencing and electron microscopy findings. We previously

Figure 2 Ultrastructural findings in cardiomyocytes. (A) Normal cardiomyocytes of a patient with dilated cardiomyopathy, without any genetic variants (40-year-old man). m, mitochondria; N, nucleus. (B) P1 with a *MYBPC3* variant (c.2833_2834delCG) had disorganized sarcomeric thick filaments (yellow arrows). The Z-line (z) remained, but some aggregates appeared club shaped. m, mitochondria. (C) P2 hosted a *TTN* nonsense variant (c.71112T>A) in exon 325, encoding the A-band domain. The M-line was absent, and sparse but organized myofilaments without thin filament were found. The Z-line (Z) structure is also maintained, and Z-line interval is constant compared with (A). m, mitochondria. (D) P4 had a *TTN* frameshift variant (c.72233delT) in exon 325 and a *DSP* missense variant (c.4996C>T). The sparse myofilament pattern is similar to (C). Diffuse myofilament lysis (ML) spreads to both sides of cell adhesion with abnormal desmosomes (red arrows). Autophagic vacuoles (AV) appeared in areas of degeneration. Li, lipofuscin; m, mitochondria. (E) P5 had a *TTN* frameshift variant (c.14488_14491delCAGT) in exon 45, encoding the I-band domain. The cardiomyocytes contained focal areas of disrupted sarcomeric structure (yellow asterisks) with lipid droplets (L). The nucleus (N) showed a normal form. m, mitochondria. (F) Higher magnification of (E) shows that thick myofilaments (yellow arrows) scatter to several directions. The boundary is unclear and includes fewer glycogen granules (g) and mitochondria (m) than surrounding areas of cardiomyocytes. Lipid droplets (L) are a finding suggestive of acute myocardial damage.[16] Li, lipofuscin; m, mitochondria. (G) In cardiomyocytes of P8 with a *TMEM43* variant (c.271A>G), diffuse myofilament lysis (ML) spreads near the abnormal-shaped nucleus (N). Scale bars = 2 μm (A, C), 1 μm (B), 5 μm (D, E, G), and 500 nm (F).
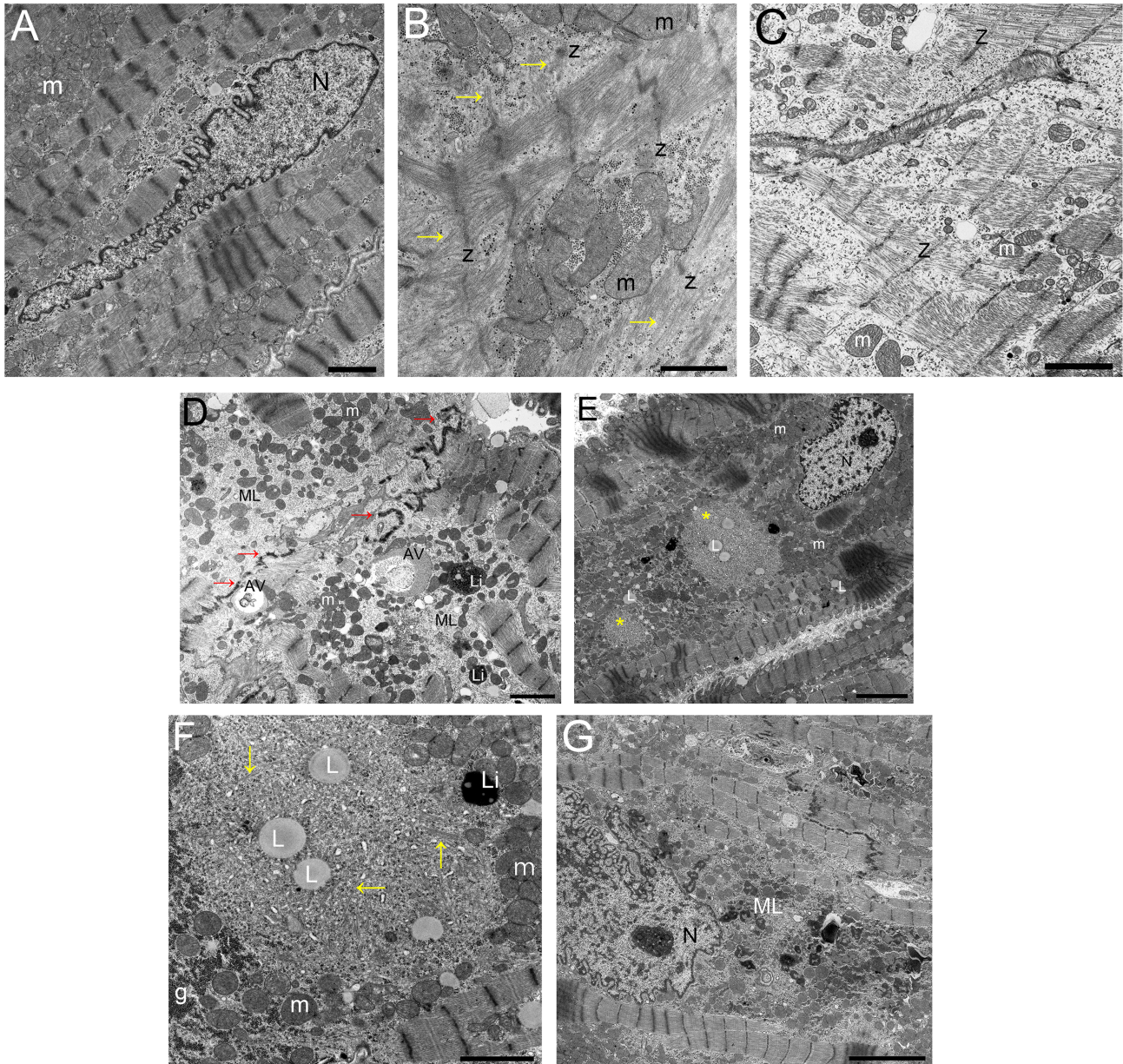
Figure 3 Ultrastructural findings in cardiomyocytes of patients with clinical manifestations of dilated cardiomyopathy. (A) At end-stage heart failure, cardiomyocytes of P1 with a *MYBPC3* variant (c.2833_2834delCG) showed severe ultrastructural changes, such as abnormally shaped nuclei (N), diffuse myofilament lysis (ML) with autophagic vacuoles (AV) of various sizes and lipofuscins (Li). (B) P7 hosted a *TMEM43* variant (c.271A>G). In the cardiomyocytes, mitochondrial hyperplasia (m) spreads to replace areas of myofilament disappearance, including degenerated mitochondrion (bold yellow arrows). AV, autophagic vacuole; L, lipid droplet. (C) In cardiomyocytes of P7, mitophagy is observed; an autophagic vacuole with a double membrane structure (surrounded by yellow arrowheads) envelops the abnormal mitochondrion (m) with swelling cristae. L, lipid droplet. Scale bar = 5 μm (A) and 2 μm (B, C).
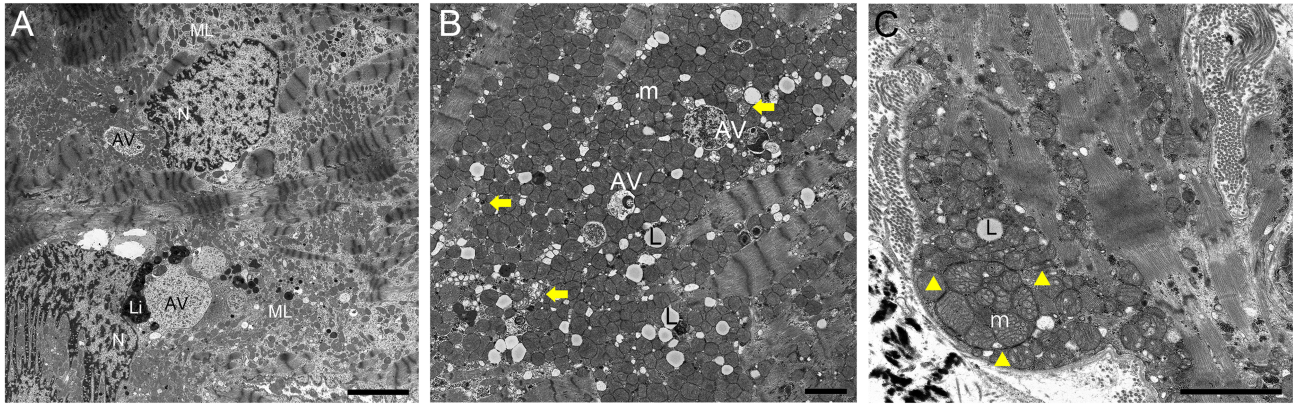
showed that DCM patients with myofilament changes in LV cardiomyocytes had poor prognosis[7] and difficulty recovering cardiac function.[16] Myofilament changes were classified as either focal derangement of myofilaments (sarcomere damage) or diffuse myofilament lysis (disappearance of most sarcomeres in cardiomyocytes).[7] In the present study, five patients with sarcomere-related gene variants were classified as P/LP; four of them (80%) showed focal myofilament derangement, and the ultrastructural findings were consistent for each gene variant. Our patient with a *MYBPC3* variant (c.2833_2834delCG) had cardiomyocytes with disorganized myofilaments with Z-band and thin filaments remaining (*Figure 2B*). This is reminiscent of the electron microscopy findings of skeletal muscle sarcomeres in patients with myopathy associated with a *MYBPC3* variant (c.2882C>T).[17] Cardiac myosin-binding protein C binds to myosin filaments, consistent with the disorganization of thick filaments in cardiomyocytes, which appear to be myosin filaments. Titin is the largest human protein (33 000 amino acids), and a variety of ultrastructural forms have been reported because of *TTN* variants.[18] Three of our patients had variants in exon 325 of *TTN*, which encodes the A-band domain of titin.[15] In those patients, electron microscopy revealed that the area around the M-line was unclear, and thick filaments became sparse with a loss of thin filaments (*Figure 2C*). One patient had a variant in exon 45, encoding an I-band domain[15] between the Z-line and A-band. In addition to sparse sarcomeres, this patient's cardiomyocytes had small focal areas of disrupted sarcomere (*Figure 2E*) where scattered bundles of thick filaments were oriented in random directions (*Figure 2F*). These were similar to the ultrastructural findings in the skeletal muscle of patients with titin-related myopathy

with mutations in the titin A-band and I-band domains, respectively.[18]

Diffuse myofilament lysis has previously been recognized in acute myocarditis due to Coxsackie virus infection[19] and in doxorubicin-induced cardiomyopathy.[20] It was considered to be a non-specific change due to various causes rather than as a result of the spread of focal myofilament derangement. We identified diffuse myofilament lysis in DCM associated with non-sarcomere-related gene variants, such as *TMEM43* and *DSP*. Even in a patient with a *MYBPC3* variant (P1), diffuse myofilament lysis was shown in cardiomyocytes obtained by EMB at the time of progressing to end-stage HF despite not being observed at the onset of HF (*Figure 3A*). Therefore, we consider diffuse myofilament lysis as an indication of a process leading to cardiomyocyte failure. In cardiomyocytes of patients with *TMEM43* variants, diffuse myofilament lysis spreads around the nuclei (*Figure 2H*). *TMEM43* encodes Luma, a nuclear membrane protein that transmits mechanical force from the cytoplasm to the nuclei, like Emerin and Lamin A/C.[21] In contrast, patients with *DSP* variants had diffuse myofilament lysis in the periphery of cardiomyocytes, with abnormal cell adhesion on both sides (*Figure 2D*). *DSP* codes for desmoplakin, which is one of the proteins that make up the outer dense plaque of desmosomes. At the onset of HF in DCM patients, distribution patterns of diffuse myofilament lysis in cardiomyocytes correlate with variants in known causative genes.

When HF occurs and DCM is diagnosed, optimal treatment commences. Some DCM patients had improved cardiac function and elimination of HF symptoms by treatments to reduce mechanical overload.[2] However, myocardial damage due to DCM may develop if there are underlying factors, like

pathogenic gene variants, and there is subsequent exposure to triggering factors, such as mechanical stress.[22] A randomized study indicated that HF symptoms and cardiac dysfunction relapse could be triggered by withdrawing optimal treatment after initial improvement of symptoms.[23] This indicates that myocardial damage in DCM can progress subclinically, even after HF improves and cardiac function recovers. A genotype–phenotype correlation has begun to show that DCM caused by *LMNA* variants has a poorer prognosis than sarcomere-related gene variants.[4,6] However, our patient with a *MYBPC3* variant (P1) had intractable HF, and ultrastructural changes in cardiomyocytes reflected severe disease progression. The present study suggests that DCM involves several conditions caused by variants in known disease-causing genes. Clarifying the causative gene in each DCM patient might inform early decision on intervention methods, such as medication, mechanical therapy, or HTx.

The current medical approach for DCM is diagnosis based on the clinical phenotype and providing treatment for HF according to symptoms. This runs the risk of delaying care for DCM due to time spent excluding other causes of cardiac dysfunction, or giving priority to treatment of co-morbidities. For example, patient P7 also had vasospastic angina and paroxysmal atrial fibrillation. As such, priority was given to treating these co-morbidities and considering these as the cause of HF at her initial admission. Beta-blockers and diuretics were not introduced, resulting in a significant delay to the treatment of HF, which may have affected the subsequent outcome of progression to HTx. P7 had an LP variant in *TMEM43* (c.271A>G). Electron microscopy revealed expanded areas of myofilament loss replaced by mitochondrial hyperplasia. There were also various abnormal mitochondrial lesions and mitophagy (*Figure 3B* and *3C*). *TMEM43* is one of the causative genes of arrhythmogenic cardiomyopathy, and there is a risk of sudden cardiac death, even with VUS.[24] If the gene variant was known at the time of diagnosis, earlier consideration could have been given to treatment, including HTx. While electron microscopy findings are still developing as evidence to judge myocardial damage and might carry a risk of overestimation when considered alone, findings with established evidence, such as myofilament changes[7] and mitochondrial abnormalities,[25] which can be readily determined, become helpful in diagnosis. We propose using ultrastructural findings as supporting evidence to determine if gene variants are pathogenic.

Study limitations

A considerable number of patients refused to have DNA collected, resulting in a smaller number of subjects and a higher proportion (47%) of severe HF patients (New York Heart Association Scale III or IV). Although providing epidemiological information was not the purpose of the present study, this selection bias is a major limitation. The small number of patients in this study prevented the statistical analysis for associations with prognosis or cardiac function. The limitations of EMB are well known,[26] particularly considering the complexity of ultrastructural interpretation and the small size of the electron microscopy field.[7,9,16] Because molecular analysis with DNA/RNA extraction was not performed in all patients, it cannot be completely ruled out that cardiomyopathy secondary to viral myocarditis was included. We think that further studies with increased numbers will elucidate the specific ultrastructural features for each gene variant.

Conclusions

While diffuse myofilament lysis in cardiomyocytes of DCM patients may be a non-specific finding, derangement pattern of myofilament and subcellular distribution of myofilament lysis might implicate particular causal genes. Future, large-scale studies are required to clarify the relationship between ultrastructural findings and the causative genes of DCM.

Acknowledgements

Conflict of interest

None declared.

Funding

References

1. Rapezzi C, Arbustini E, Caforio AL, Charron P, Gimeno-Blanes J, Heliö T, Linhart A, Mogensen J, Pinto Y, Ristic A, Seggewiss H, Sinagra G, Tavazzi L, Elliott PM. Diagnostic work-up in cardiomyopathies: bridging the gap between clinical phenotypes and final diagnosis. A position statement from the ESC Working Group on Myocardial and Pericardial Diseases. *Eur Heart J* 2013; **34**: 1448–1458.

2. Merlo M, Pyxaras SA, Pinamonti B, Barbati G, Di Lenarda A, Sinagra G. Prevalence and prognostic significance of left ventricular reverse remodeling in dilated cardiomyopathy receiving tailored medical treatment. *J Am Coll Cardiol* 2011; **57**: 1468–1476.

3. Herman DS, Lam L, Taylor MR, Wang L, Teekakirikul P, Christodoulou D, Conner L, DePalma SR, McDonough B, Sparks E, Teodorescu DL, Cirino AL, Banner NR, Pennell DJ, Graw S, Merlo M, Di Lenarda A, Sinagra G, Bos JM, Ackerman MJ, Mitchell RN, Murry CE, Lakdawala NK, Ho CY, Barton PJ, Cook SA, Mestroni L, Seidman JG, Seidman CE. Truncations of titin causing dilated cardiomyopathy. *N Engl J Med* 2012; **366**: 619–628.

4. Hasselberg NE, Haland TF, Saberniak J, Brekke PH, Berge KE, Leren TP, Edvardsen T, Haugaa KH. Lamin A/C cardiomyopathy: young onset, high penetrance, and frequent need for heart transplantation. *Eur Heart J* 2018; **39**: 853–860.

5. Akinrinade O, Ollila L, Vattulainen S, Tallila J, Gentile M, Salmenperä P, Koillinen H, Kaartinen M, Nieminen MS, Myllykangas S, Alastalo TP, Koskenvuo JW, Heliö T. Genetics and genotype–phenotype correlations in Finnish patients with dilated cardiomyopathy. *Eur Heart J* 2015; **36**: 2327–2337.

6. Tobita T, Nomura S, Fujita T, Morita H, Asano Y, Onoue K, Ito M, Imai Y, Suzuki A, Ko T, Satoh M, Fujita K, Naito AT, Furutani Y, Toko H, Harada M, Amiya E, Hatano M, Takimoto E, Shiga T, Nakanishi T, Sakata Y, Ono M, Saito Y, Takashima S, Hagiwara N, Aburatani H, Komuro I. Genetic basis of cardiomyopathy and the genotypes involved in prognosis and left ventricular reverse remodeling. *Sci Rep* 2018; **8**: 1998.

7. Saito T, Asai K, Sato S, Takano H, Mizuno K. Ultrastructural features of cardiomyocytes in dilated cardiomyopathy with initially decompensated heart failure as a predictor of prognosis. *Eur Heart J* 2015; **36**: 724–733.

8. Kanzaki M, Asano Y, Ishibashi-Ueda H, Oiki E, Nishida T, Asanuma H, Kato H, Oka T, Ohtani T, Tsukamoto O, Higo S, Kioka H, Matsuoka K, Sawa Y, Komuro I, Kitakaze M, Takashima S, Sakata Y. A development of nucleic chromatin measurements as a new prognostic marker for severe chronic heart failure. *PLoS One* 2016; **11**: e0148209.

9. Saito T, Asai K, Sato S, Hayashi M, Adachi A, Sasaki Y, Takano H, Mizuno K, Shimizu W. Autophagic vacuoles in cardiomyocytes of dilated cardiomyopathy with initially decompensated heart failure predict improved prognosis. *Autophagy* 2016; **12**: 579–587.

10. Castelli G, Fornaro A, Ciaccheri M, Dolara A, Troiani V, Tomberli B, Olivotto I, Gensini GF. Improving survival rates of patients with idiopathic dilated cardiomyopathy in Tuscany over 3 decades: impact of evidence-based management. *Circ Heart Fail* 2013; **6**: 913–921.

11. Pearce C, Goettke E, Hallowell N, McCormack P, Flinter F, McKevitt C. Delivering genomic medicine in the United Kingdom National Health Service: a systematic review and narrative synthesis. *Genet Med* 2019; **21**: 2667–2675.

12. Schiller NB, Shah PM, Crawford M, DeMaria A, Devereux R, Feigenbaum H, Gutgesell H, Reichek N, Sahn D, Schnittger I. Recommendations for quantitation of the left ventricle by two-dimensional echocardiography. American Society of Echocardiography Committee on Standards, Subcommittee on Quantitation of Two-Dimensional Echocardiograms. *J Am Soc Echocardiogr* 1989; **2**: 358–367.

13. Hershberger RE & Morales A GeneRevies: dilated cardiomyopathy overview. https://www.ncbi.nlm.nih.gov/books/NBK1309/ Accessed October 15, 2020.

14. Morales A, Kinnamon DD, Jordan E, Platt J, Vatta M, Dorschner MO, Starkey CA, Mead JO, Ai T, Burke W, Gastier-Foster J, Jarvik GP, Rehm HL, Nickerson DA, Hershberger RE, DCM Precision Medicine study of the DCM Consortium. Variant interpretation for dilated cardiomyopathy: refinement of the American College of Medical Genetics and Genomics/ClinGen guidelines for the DCM Precision Medicine Study. *Circ Genom Precis Med* 2020; **13**: 43–51.

15. Labeit S, Lahmers S, Burkart C, Fong C, McNabb M, Witt S, Witt C, Labeit D, Granzier H. Expression of distinct classes of titin isoforms in striated and smooth muscles by alternative splicing, and their conserved interaction with filamins. *J Mol Biol* 2006; **362**: 664–681.

16. Saito T, Asai K, Tachi M, Sato S, Mozawa K, Adachi A, Sasaki Y, Amano Y, Mizuno K, Kumita SI, Shimizu W. Long-term prognostic value of ultrastructural features in dilated cardiomyopathy: comparison with cardiac magnetic resonance. *ESC Heart Fail* 2020; **7**: 682–691.

17. Tajsharghi H, Leren TP, Abdul-Hussein S, Tulinius M, Brunvand L, Dahl HM, Oldfors A. Unexpected myopathy associated with a mutation in *MYBPC3* and misplacement of the cardiac myosin binding protein C. *J Med Genet* 2010; **47**: 575–577.

18. Ávila-Polo R, Malfatti E, Lornage X, Cheraud C, Nelson I, Nectoux J, Böhm J, Schneider R, Hedberg-Oldfors C, Eymard B, Monges S, Lubieniecki F, Brochier G, Thao Bui M, Madelaine A, Labasse C, Beuvin M, Lacène E, Boland A, Deleuze JF, Thompson J, Richard I, Taratuto AL, Udd B, Leturcq F, Bonne G, Oldfors A, Laporte J, Romero NB. Loss of sarcomeric scaffolding as a common baseline histopathologic lesion in titin-related myopathies. *J Neuropathol Exp Neurol* 2018; **77**: 1101–1114.

19. Ikeda T, Saito T, Takagi G, Sato S, Takano H, Hosokawa Y, Hayashi M, Asai K, Yasutake M, Mizuno K. Acute myocarditis associated with coxsackievirus B4 mimicking influenza myocarditis: electron microscopy detection of causal virus of myocarditis. *Circulation* 2013; **128**: 2811–2812.

20. Takemura G, Onoue K, Nakano T, Nakamura T, Sakaguchi Y, Tsujimoto A, Miyazaki N, Watanabe T, Kanamori H, Okada H, Kawasaki M, Fujiwara T, Fujiwara H, Saito Y. Possible mechanism for disposal of degenerative cardiomyocytes in human failing hearts: phagocytosis by a neighbour. *ESC Heart Fail* 2019; **6**: 208–216.

21. Stroud MJ, Banerjee I, Veevers J, Chen J. Linker of nucleoskeleton and cytoskeleton complex proteins in cardiac structure, function, and disease. *Circ Res* 2014; **114**: 538–548.

22. Nomura S, Satoh M, Fujita T, Higo T, Sumida T, Ko T, Yamaguchi T, Tobita T, Naito AT, Ito M, Fujita K, Harada M, Toko H, Kobayashi Y, Ito K, Takimoto E, Akazawa H, Morita H, Aburatani H, Komuro I. Cardiomyocyte gene programs encoding morphological and functional signatures in cardiac hypertrophy and failure. *Nat Commun* 2018; **9**: 4435.

23. Halliday BP, Wassall R, Lota AS, Khalique Z, Gregson J, Newsome S, Jackson R, Rahneva T, Wage R, Smith G, Venneri L, Tayal U, Auger D, Midwinter W, Whiffin N, Rajani R, Dungu JN, Pantazis A, Cook SA, Ware JS, Baksi AJ, Pennell DJ, Rosen SD, Cowie MR, Cleland JGF, Prasad SK. Withdrawal of pharmacological treatment for heart failure in patients with recovered dilated cardiomyopathy (TRED-HF): an open-label, pilot, randomised trial. *Lancet* 2019; **393**: 61–73.

24. Fressart V, Duthoit G, Donal E, Probst V, Deharo JC, Chevalier P, Klug D, Dubourg O, Delacretaz E, Cosnay P, Scanu P, Extramiana F, Keller D, Hidden-Lucet F,

Simon F, Bessirard V, Roux-Buisson N, Hebert JL, Azarine A, Casset-Senon D, Rouzet F, Lecarpentier Y, Fontaine G, Coirault C, Frank R, Hainque B, Charron P. Desmosomal gene analysis in arrhythmogenic right ventricular dysplasia/cardiomyopathy: spectrum of mutations and clinical impact in practice. *Europace* 2010; **12**: 861–868.

25. Arbustini E, Diegoli M, Fasani R, Grasso M, Morbini P, Banchieri N, Bellini O, Dal Bello B, Pilotto A, Magrini G, Campana C, Fortina P, Gavazzi A, Narula J, Viganò M. Mitochondrial DNA mutations and mitochondrial abnormalities in dilated cardiomyopathy. *Am J Pathol* 1998; **153**: 1501–1510.

26. Mason JW, O'Connell JB. Clinical merit of endomyocardial biopsy. *Circulation* 1989; **79**: 971–979.